



## Strain visualization enabled in dual-wavelength InGaN/GaN multiple quantum wells Micro-LEDs by piezo-phototronic effect

Yu Yin<sup>a,b,c,1</sup>, Renfeng Chen<sup>a,b,1</sup>, Rui He<sup>a,b</sup>, Yiwei Duo<sup>a,b</sup>, Hao Long<sup>c,\*</sup>, Weiguo Hu<sup>d</sup>, Junyi Zhai<sup>d</sup>, Caofeng Pan<sup>d</sup>, Zihui Zhang<sup>e</sup>, Junxi Wang<sup>a,b</sup>, Jinmin Li<sup>a,b</sup>, Tongbo Wei<sup>a,b,\*\*</sup>

<sup>a</sup> Research and Development Center for Semiconductor Lighting Technology, Institute of Semiconductors, Chinese Academy of Sciences, Beijing 100083, China

<sup>b</sup> Center of Materials Science and Optoelectronics Engineering, University of Chinese Academy of Sciences, Beijing 100049, China

<sup>c</sup> School of Electronic Science and Engineering (National Model Microelectronics College), Xiamen University, Xiamen 361005, China

<sup>d</sup> CAS Center for Excellence in Nanoscience, Beijing Key Laboratory of Micro-nano Energy and Sensor, Beijing Institute of Nanoenergy and Nanosystems, Chinese Academy of Sciences, Beijing 100083, China

<sup>e</sup> School of Integrated Circuits, Guangdong University of Technology, 100 Waihuan West Road, Fanyu District, Guangzhou City, Guangdong Province, 510006, China

### ARTICLE INFO

#### Keywords:

Dual-wavelength MQWs  
Micro-LEDs  
Optical strain sensor  
Piezo-phototronic effect  
Display color change

### ABSTRACT

Optical strain sensor for stress visualization is a significant topic in biomechanical imaging or electronic skin. In this study, the dual-wavelength InGaN/GaN multiple-quantum-wells (MQWs) micro light emitting diode (Micro-LED) is demonstrated with color response under mechanical stimulation by piezo-phototronic effect. The peak intensity of green light increases by about 37%, while the blue decreases by 10% at the external strain of 0.20%. Simultaneously, the intensity integral ratio of green and blue light changes from 43:57–53:47, leading to the display color shift from light blue to turquoise significantly. It is noted that electrical injection shows a greater color response than photoluminescence, indicating that the piezo-phototronic effect changes both the recombination in MQWs and the carrier injection. The different piezoelectric modulation between green QW and blue QW lies on the different strain-induced piezoelectric polarized charges in the interface of InGaN QWs, revealed by experiments and APSYS simulation in details. This study is of high significance for the development of optical-based stress sensor with strain visualization and high spatial resolution for smart sensing and micro-opto-electromechanical systems.

### 1. Introduction

Tactile and pressure sensors with micro/nano structures are significant in the fields of wearable electronics and human-machine interfaces [1–3]. Wearable strain sensors normally have effective electromechanical responses to external stimuli [4,5]. And various pressure sensors have been designed based on nanowires/nanotubes [6,7], polymer composite dielectric [8,9], organic thin film [10], and demonstrated to have a high sensitivity. However, the electronic responses of pressure sensors are limited by parasitic resistance or capacitance, especially when considering the integration of large number of micro-/nano-sized sensors [11]. With the increasing density and decreasing size of sensors, the sensitivity decreases accompanied by undesired and severe

crosstalk, which makes it difficult in the detection of pressure in microscale. Alternatively, owing to the fast response time and high sensitivity of optical devices, the coupling of force-electricity-optical signals in pressure sensors attracts great attention [12–14]. The optical pressure sensor based on light emitting diode (LED) arrays is capable in sensing the external pressure changes by analyzing the variation of optical signals [15]. Furthermore, by the collection of spatial optical signals of miniaturized optical sensors, high spatial resolution pressure mapping could be realized, which achieves stress visualization [16,17]. Thus, strain detection based on photonic sensing with high resolution and fast response is of high significance for Internet of things (IoT).

InGaN/GaN multiple-quantum-wells (MQWs) are the most widely applied light emitting structure for photonic devices, which have been

\* Corresponding author.

\*\* Corresponding author at: Research and Development Center for Semiconductor Lighting Technology, Institute of Semiconductors, Chinese Academy of Sciences, Beijing 100083, China.

E-mail addresses: [longhao@xmu.edu.cn](mailto:longhao@xmu.edu.cn) (H. Long), [tbwei@semi.ac.cn](mailto:tbwei@semi.ac.cn) (T. Wei).

<sup>1</sup> Yu Yin and Renfeng Chen contributed equally.

developed in illumination and visible light communication. Due to the non-centrosymmetric structure of wurtzite nitride crystals, the piezoelectric potential could be induced by various external strain in group III nitride such as GaN, AlN, InN [18–20]. With the modulation of the internal piezoelectric field by the strain-induced interface polarized charges, the light emitting properties could be changed in InGaN/GaN MQWs [21,22]. This strain-to-light signal response is essentially modulated by the energy band structure under different strain condition, which has been defined as piezo-phototronic effect with the three-way coupling among semiconductor properties, piezoelectric polarization, and optical excitation [23,24]. The effective band gap and the electron-hole wavefunction overlap ratio in InGaN/GaN MQWs could be changed via the application of in-plane biaxial stress, resulting in a variation of luminous intensity and wavelength [25,26]. Recently, most reports focused on the changes in the single wavelength emission intensity of InGaN/GaN MQWs under different strain condition [27–29], but the collection of light intensity is susceptible by optical deviation, which leads to the decrease in sensing accuracy. The wavelength shift could provide a more reliable information in strain-optical sensing and it has great potential for the realization of strain visualization. However, the wavelength shift of single wavelength InGaN/GaN MQWs is normally limited under different compressive or tensile strain, which is usually about few nanometers ( $\sim 2$  nm at a strain of 1%) [30,31]. Furthermore, dual-wavelength InGaN/GaN MQWs with micro-structure has the potential of optical response to mechanical stimuli [32], but the wavelength response has not been studied up to now. The piezo-phototronic modulation mechanism in dual-wavelength InGaN/GaN MQWs remains rarely explored in current studies, while it is crucial for the display color shift in dual-wavelength MQWs.

In this work, we propose a stress visualized optical strain sensor based on dual-wavelength InGaN/GaN MQWs micro light emitting diode (Micro-LED). The dual peak wavelengths are located at about 450 nm and 550 nm, respectively, by designing the sandwich structure of

short-wavelength quantum wells (QWs) and long-wavelength single quantum well (SQW) grown on sapphire substrate. The stress and optical properties are studied at different strain condition via Raman scattering spectra, photoluminescence (PL) and electroluminescence (EL) experiments. It is found the integral intensity ratio of green and blue peak changes from 43:57–53:47 with increasing external in-plane tensile strain up to 0.20%, leading to the shift in the displayed color from light blue to turquoise. The modulation in the dynamics behavior of carriers in MQWs under piezo-phototronic effect is revealed combining the time-resolution photoluminescence (TRPL) and APSYS simulation. This result provides the guidance for optical strain sensor with a high spatial resolution and strain visualization in the field of wearable electronics and human-machine interfaces.

## 2. Experimental section

The dual-wavelength InGaN/GaN MQWs LEDs are grown on c-plane (0001) sapphire substrate by metal organic chemical vapor deposition (MOCVD). As shown in Fig. 1(a), the epitaxial structure includes a low-temperature nucleation layer, Si-doped n-GaN layer, a six-period  $\text{In}_x\text{Ga}_{1-x}\text{N}/\text{GaN}$  MQWs structure and Mg-doped p-GaN layer. Specifically, the  $\text{In}_x\text{Ga}_{1-x}\text{N}/\text{GaN}$  MQWs structure is composed of five periods of blue MQWs and one period of green SQW. And the green QW is located between the first and the second blue QW from the top to bottom. It is noted that a thin GaN barrier with one-half thickness of normal barrier is inserted between the first blue QW and the green QW. The design of first blue QW and thin GaN quantum barrier (QB) are aimed at increasing the hole injection from p-GaN to the green QW, which is conducive to the dual wavelength emission of MQWs.

The Micro-LED arrays are fabricated using standard processing techniques. The micropillars with  $60 \mu\text{m}$  are prepared by inductively coupled plasma (ICP). Then Ti/Al/Ni/Au (20 nm/60 nm/30 nm/100 nm) multilayer metals are deposited on the n-GaN by electron beam

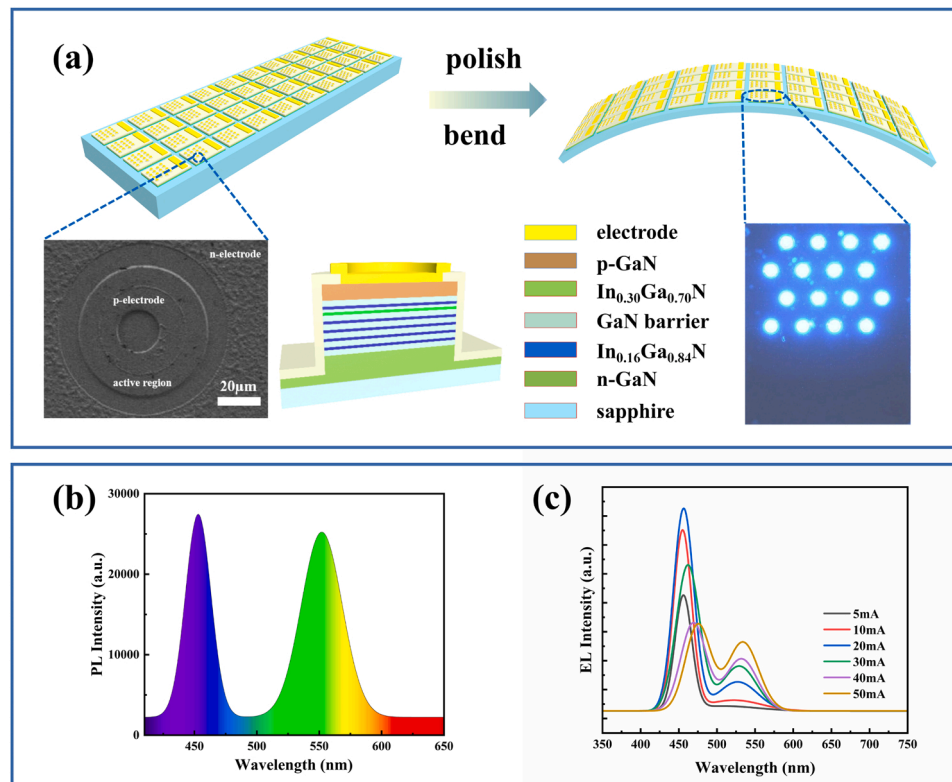


**Fig. 1.** (a) Schematic diagram of the dual-wavelength MQWs structure and the fabrication of flexible Micro-LED arrays. The illustration is the SEM image of single pillar (the left) and the luminous image of Micro-LED arrays (the right). (b) PL spectra of dual-wavelength InGaN/GaN MQWs. (c) EL spectra of dual-wavelength Micro-LED arrays under different injection current.

evaporation. Annealing at 1000 °C for 30 s in N<sub>2</sub> atmosphere is applied to form ohmic contact. Similarly, the p-GaN region sputters the Ni/Au (30 nm/150 nm) and is annealed at 700 °C for 1 min in N<sub>2</sub> atmosphere to achieve the ohmic contact in p-electrode. Next, 1100 nm thickness SiO<sub>2</sub> layer is deposited by plasma-enhanced vapor deposition (PECVD) to form the passivation layer and using wet etching to bare the n-electrode and p-electrode hereafter. The Al/Ti/Au (1700 nm/50 nm/300 nm) layers are deposited on the exposed electrodes. Finally, the top of the wafer is coated wax to protect the electrode and then the sapphire substrate is horizontally thinned and polished to 80 μm in order to easily apply bending strain and is divided into strip with the size of 1 cm × 0.5 cm by laser scribing. The scanning electron microscope (SEM) image of single pillar and the luminous image of Micro-LED arrays are shown in Fig. 1(c). The fabricated dual-wavelength Micro-LED arrays exhibit two emitting peaks about 450 nm and 550 nm in PL spectra, respectively, as shown in Fig. 1(b). At different injected current, the EL spectra also show the dual-wavelength characteristics in Fig. 1(c). With the increase of injection current, the intensity of green peak rapidly enhances, producing phosphor-free white light emission. In contrast, the intensity of blue peak instead decreases due to the overflow of electrons at high current.

### 3. Results and discussion

The stress condition has been discussed by Raman scattering spectra with a customized experimental setup in Fig. 2(a) when applying different strain. Due to the reduced in-plane compressive stress of the epitaxial layer from the thinned substrate after polishing the sapphire substrate, the sample bends upward slightly and spontaneously [33]. By changing the horizontal compression, the thinned samples could bend

upward in different degrees, indicating different in-plane tensile strain has been introduced into the Micro-LED epi-layer. It has been demonstrated that uniform strain is induced in the large area of bending sample [26]. The conversion relationship between horizontal compression and tensile strain is shown in supporting information S1 and the results are shown in Fig. 2(b). Through changing compression from 0 μm to 100 μm, the external tensile strain increases to about 0.20%, which is of high precision for the piezo-phototronic modulation of InGaN/GaN MQWs. Normally, the InGaN QWs suffer from in-plane compressive strain caused by both the mismatch between InGaN QWs and GaN QBs and the stress from sapphire substrate. This strain induces the piezoelectric polarized charges in the interface of InGaN/GaN MQWs, which results in a large built-in electric field and affects the light emission in QWs [34]. In order to evaluate the stress condition in InGaN/GaN MQWs with different external tensile strain, the shift of GaN E<sub>2,high</sub> Raman mode is characterized which represents the average stress in the epi-layer. As shown in Fig. 2(c), the E<sub>2,high</sub> Raman peak shifts to short wavenumber from 569.78 cm<sup>-1</sup> to 567.8 cm<sup>-1</sup> with the increasing external strain, meaning that the in-plane compressive strain decreases. This reveals the compensation effect of external strain on internal strain in the InGaN/GaN MQWs. The residual stress change can be estimated by the biaxial strain model with the following formula [35]:

$$\Delta\sigma = \Delta\omega/K \quad (1)$$

where  $\Delta\sigma$  is the in-plane biaxial stress,  $\Delta\omega = \omega - \omega_0$  is the relative offset of E<sub>2,high</sub> Raman peak ( $\omega_0 = 568 \text{ cm}^{-1}$  is the standard peak of strain-free GaN), and K is the biaxial stress coefficient ( $K = 4.2 \text{ cm}^{-1} \text{ GPa}^{-1}$  for GaN). As shown in Fig. 2(d), large residual stress about 419 MPa can be deduced from Eq. (1) at the strain-free condition (0% external strain). With increasing the external tensile strain, the residual stress in Micro-

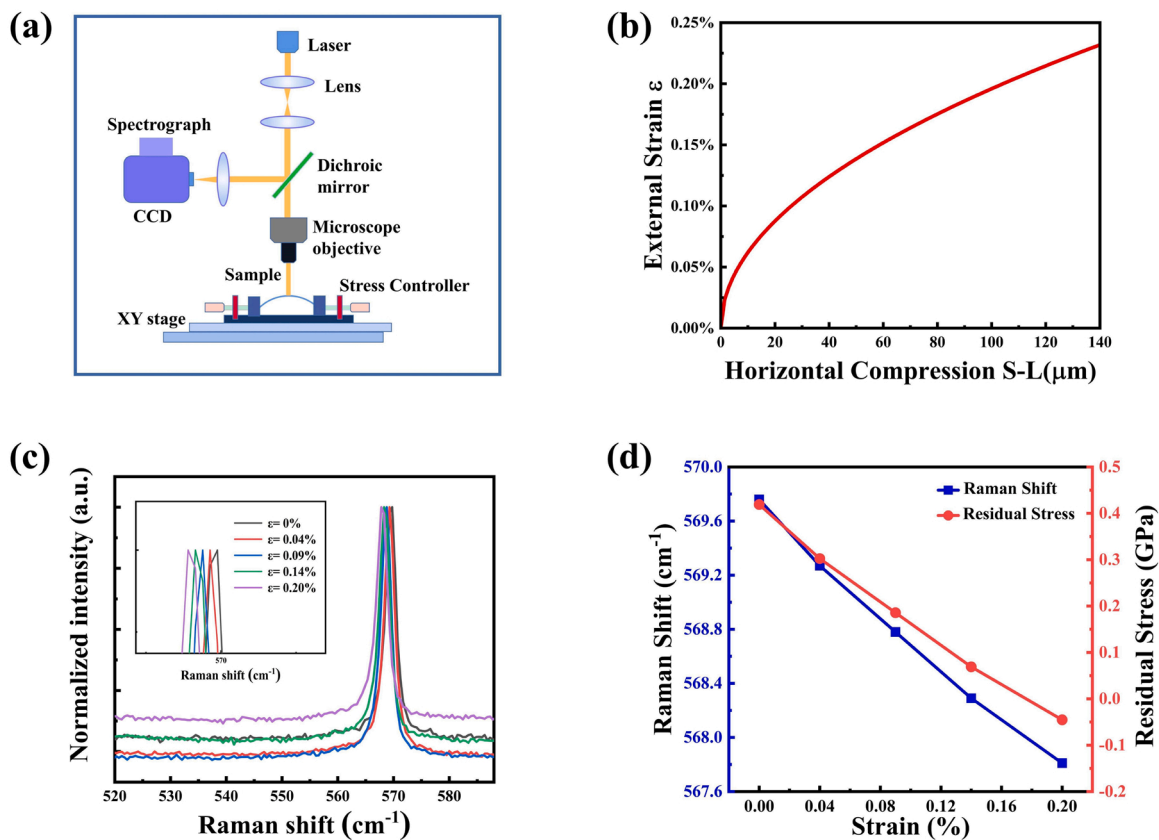


Fig. 2. (a) Schematic diagram of the Raman scattering spectra test system with stress controller. Two precision displacement devices with two Spiral Micrometers are used to fix or bend the sample, and the upward convex bending can be stably applied by the movement of displacement devices. (b) The relationship between horizontal compression and tensile strain. (c) Raman scattering spectra at different external in-plane tensile strain in dual-wavelength Micro-LED. (d) Raman peak shift and residual stress change at different external in-plane tensile strain in dual-wavelength Micro-LED.

LED epi-layer decreases significantly, which exhibits slightly tensile stress state of  $-45$  MPa at the 0.20% external strain. Therefore, tensile stress is introduced into the MQWs effectively under upward bending strain, which is conducive to the further modulation of built-in electric field in InGaN MQWs.

Fig. 3(a) shows the PL measurement at room temperature for blue and green dual-wavelength Micro-LED under various tensile strain. Owing to the In composition difference between blue QW and green QW, the force-optical response exhibits obvious discrepancy. The PL intensity of both blue and green emission increases under small strain conditions. However, when the tensile strain continues to increase after a critical value, the blue light intensity begins to decrease, while the green emission still becomes higher. With the application of in-plane tensile strain, the c-axis compressive stress is introduced into InGaN MQWs, which compensates the initial c-axis tensile stress in MQWs. It has been demonstrated that the stress compensation effect can reduce the quantum-confined Stark effect (QCSE), leading to an increase of light intensity and a blueshift in peak wavelength [36]. However, due to the larger lattice mismatch in green InGaN/GaN QW than blue InGaN/GaN QW, more external stress is needed to compensate the internal stress in green QW. This results in a larger intensity variation and wavelength shift in green InGaN/GaN SQW under different external strain, as shown in Fig. 3(b-c). The blue light reaches maximum intensity about 110% at the strain of 0.09%, while the green light may enhance to maximum intensity (128%) until a maximum external strain of 0.20% is applied. And as the strain increases from 0.09% to 0.20%, the light intensity of blue QW declines by about 9%, attributed to the stress over-compensation phenomenon in the piezo-phototronic modulation of MQWs [37]. Furthermore, it is observed that the green peak exhibits a

larger blueshift about 1.8 nm at the strain of 0.20%, while the blue peak first blueshifts and then redshifts with the increase of external strain. The wavelength shift is normally limited in InGaN/GaN MQWs experimentally in piezo-phototronic effect, even when it comes to the green light band. This is probably related to localization centers and energy band restructure modified by the strain, which include the band gap, valence band degeneracy, and effective mass of holes. It is noting that the changes in the ratio of blue and green dual-wavelength of InGaN/GaN MQWs by piezo-phototronic effect might take place of the wavelength change in single-wavelength devices [38]. As shown in Fig. 3(d), when external strain is applied, green light intensity increases and exceeds the blue with an obvious blueshift of overall waveform simultaneously. The peak intensity and integral intensity of green light significantly increase to 128% and 124%, respectively, at the strain of 0.20%, while there are few changes in the blue light. Therefore, the proportion of blue-green light emission changes in dual-wavelength InGaN/GaN MQWs under various external strain, which brings the variety of display color.

The TRPL experiments for blue light and green light of dual-wavelength InGaN/GaN MQWs are performed to further reveal the differences between the piezo-phototronic modulation of blue light and green light. As shown in Fig. 4(a) and (b), the PL decay curves exhibit non-mono-exponential behaviors both in blue QW and green QW, and all the curves can be fitted by double exponential decays. The fit constant  $\tau_1$  and  $\tau_2$ , which represent slow decay lifetime and fast decay lifetime, respectively, have a decreasing tendency under low external strain conditions. However, when the strain increases to 0.09%, the attenuation speed of the PL decay spectrum of the blue light begins to decrease, while it is still increasing for green light. The two decay

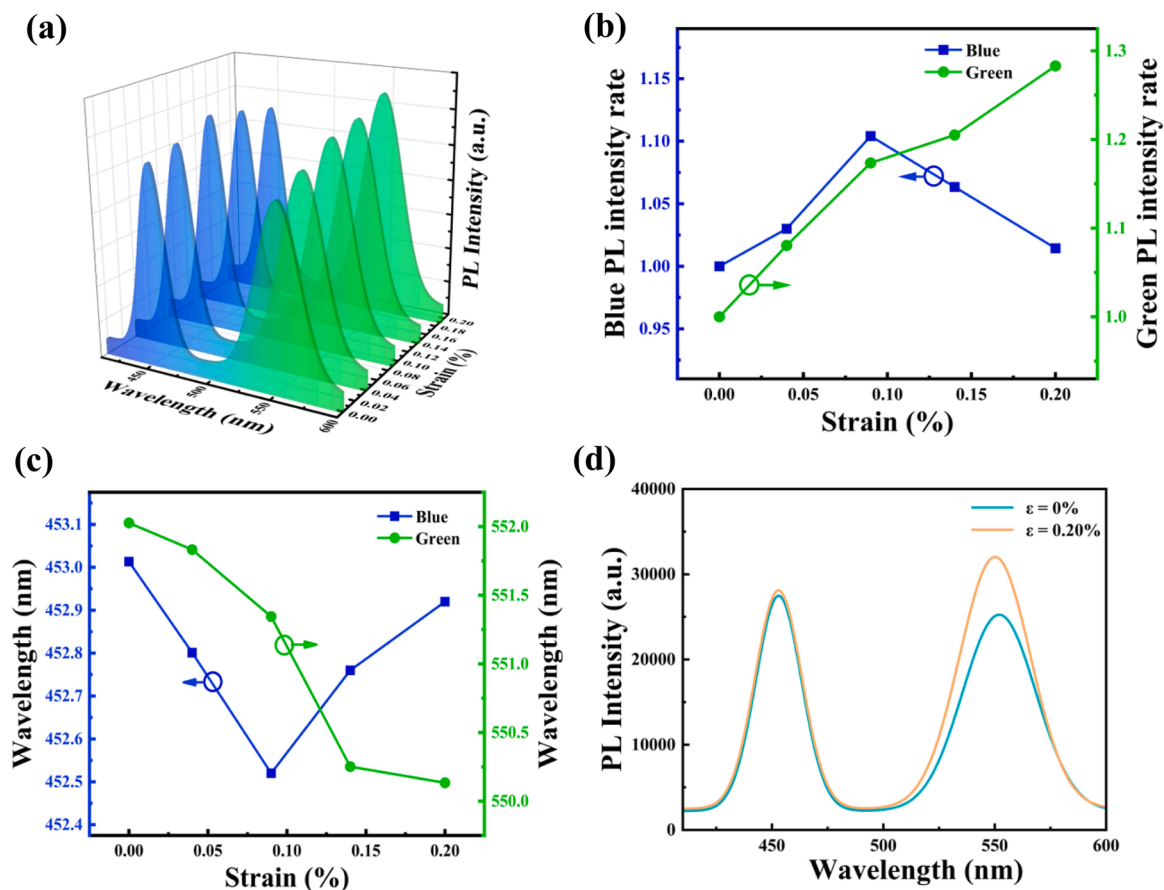


Fig. 3. (a) PL spectra of blue and green dual-wavelength InGaN/GaN MQWs Micro-LED under different external strain. (b) PL intensity and (c) peak wavelength of blue light and green light change under different external strain. (d) Peak intensity and integral intensity of blue light and green light at the external strain of 0% and 0.20% respectively.

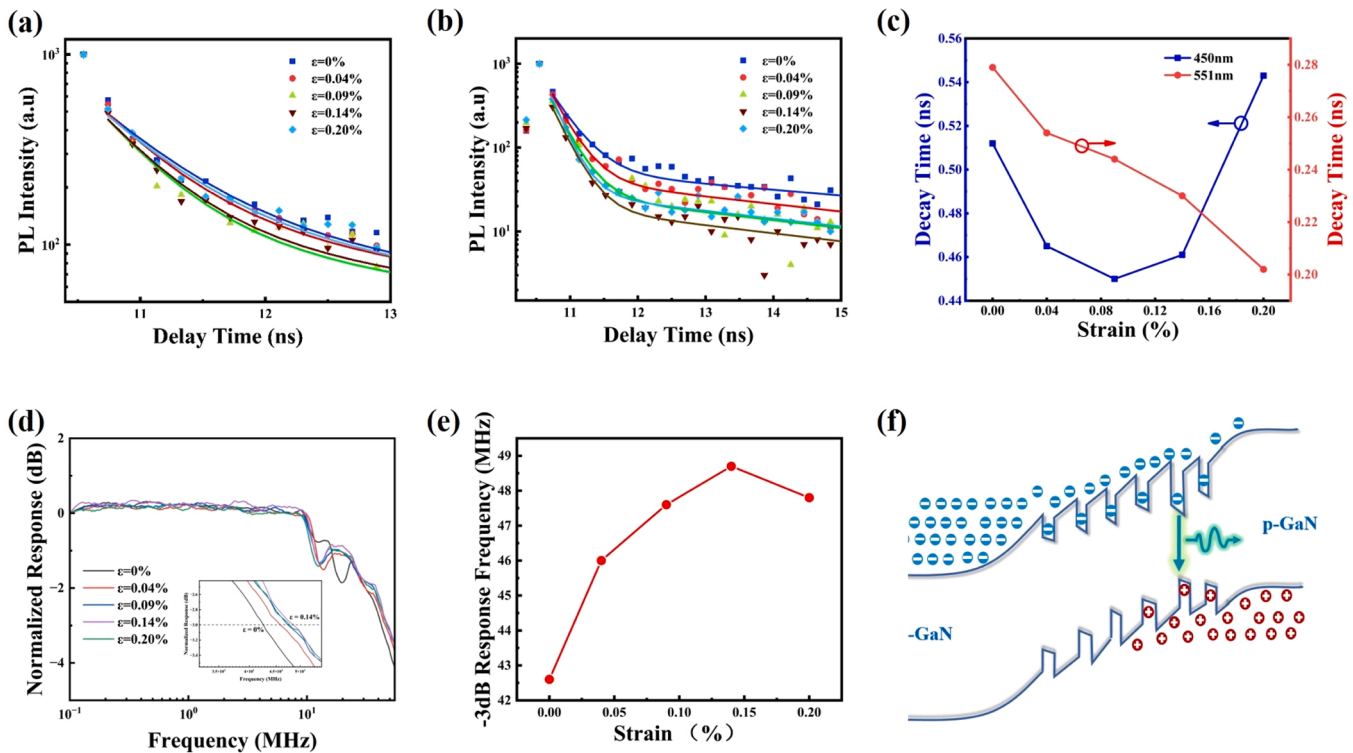


Fig. 4. TRPL spectra of (a) blue QW and (b) green QW in dual-wavelength InGaN/GaN MQWs under different external strain. (c) PL decay time of blue QW and green QW at different external bending strain. (d) Frequency responses of dual-wavelength Micro-LEDs under different strain conditions. (e) The change of  $-3$  dB modulation bandwidths with the increasing of external strain. (f) Schematic diagram of carrier injection and decay in two types of QWs.

processes are considered as the transition to strong localized states and the recombination of carriers in them respectively [39], which are highly correlated with the radiative recombination lifetime and non-radiative recombination lifetime. It can be deduced that the radiative recombination rate of excitons might increase in blue and green InGaN QW under the effect of stress compensation, which results in a higher light emission of MQWs. However, due to the less built-in piezoelectric polarization field of blue QW than green QW, the direction of the field tends to easily reverse under over-large external strain, leading to a decrease of emitting light intensity [40]. Therefore, the effective carrier lifetime  $\tau_{eff}$  first decreases (12%) and then increases (17%) for blue light, but it continues to decrease by about 28% for green light with the external strain up to 0.20% in Fig. 4(c). These results indicate that the carrier dynamics behaviors under various strain is different in blue QW and green QW, which might be caused by the dissimilarity of the stress modulation effect in energy band structure.

In order to further understand the strain-induced additional piezoelectric polarization field in blue and green QW, the piezo-phototronic modulation behaviors have been discussed in depth under the action of external electric field. Fig. 4(d) shows the  $-3$  dB modulation bandwidths of the dual-wavelength Micro-LED with different strain conditions. The modulation bandwidth is positively correlated to internal quantum efficiency (IQE) at low injection current densities [41], and it can be expressed as the reciprocal of  $\tau_{eff}$  multiplied by a constant coefficient. With the compensation effect of external in-plane tensile strain on internal compressive strain, the built-in piezoelectric field reduces and the effective carrier lifetime decreases in both blue QW and green QW. Thus, the  $-3$  dB modulation bandwidths increase as the internal residual stress declines. However, it is noting that when external strain reaches to a critical value about 0.09%, the decay time increases in blue QW but decrease in green QW. When considering these two types of QWs simultaneously, there will be competition between the two carrier lifetime contributions to the modulation bandwidth. As shown in Fig. 4 (e), the  $-3$  dB modulation bandwidths constantly increase to 113%

before the strain of 0.14% and have a slight decrease at higher external strain. Importantly, the two external strains do not coincide when the bandwidths reach the maximum and the blue light decay lifetime reaches the minimum. It may be concluded that the decrease of green light decay lifetime is dominant compared to the increase of blue light decay lifetime when the external strain is in the range of 0.09% and 0.14%. And at the higher strain than 0.14%, the attenuation of blue decay lifetime becomes the main factor. These results further demonstrate the difference of carrier dynamic behaviors between blue QW and green QW in dual-wavelength Micro-LED by piezo-phototronic effect. In addition, different from the photogenerated carriers of PL, electrical injection carriers are mainly distributed in the QWs near the p-GaN as shown in Fig. 4(f). Although the piezo-phototronic modulation is different in blue QW and green QW, the light emitting characteristic under electrical injection still need further discussion.

Fig. 5(a) shows the EL spectra of blue and green dual-wavelength Micro-LEDs under different external strain at the injected current of 20 mA. The blue light peak is obviously higher than green light peak, which is distinguished from the results of PL. But as the applied in-plane tensile strain increases, the intensity of blue light and green light exhibits the same tendency like that in PL experiments. The light intensity of blue shows an enhancement of 11% at the strain of 0.09% and then decreases by 10% at larger strain, while the green light increases by 37% under a 0.20% tensile strain in Fig. 5(b). It is noted that the EL enhancement of green light and the decline of blue light at high strain is more significant than PL, which is probably caused by the distribution of electrical injection carriers. In particular, the integral intensity ratio of green light to blue light constantly increases under the increasingly larger external strain. As shown in Fig. 5(c), the integral intensity ratio of green to blue peak increases from 43:57–53:47 as the strain increases from 0% to 0.20%, meaning that the dominated light color of Micro-LED shifts from blue to green gradually. This color change is expressed as a chromaticity coordinate shift from (0.209, 0.272) to (0.224, 0.332) in CIE chromaticity diagram, as shown in Fig. 5(d). Specifically, the EL

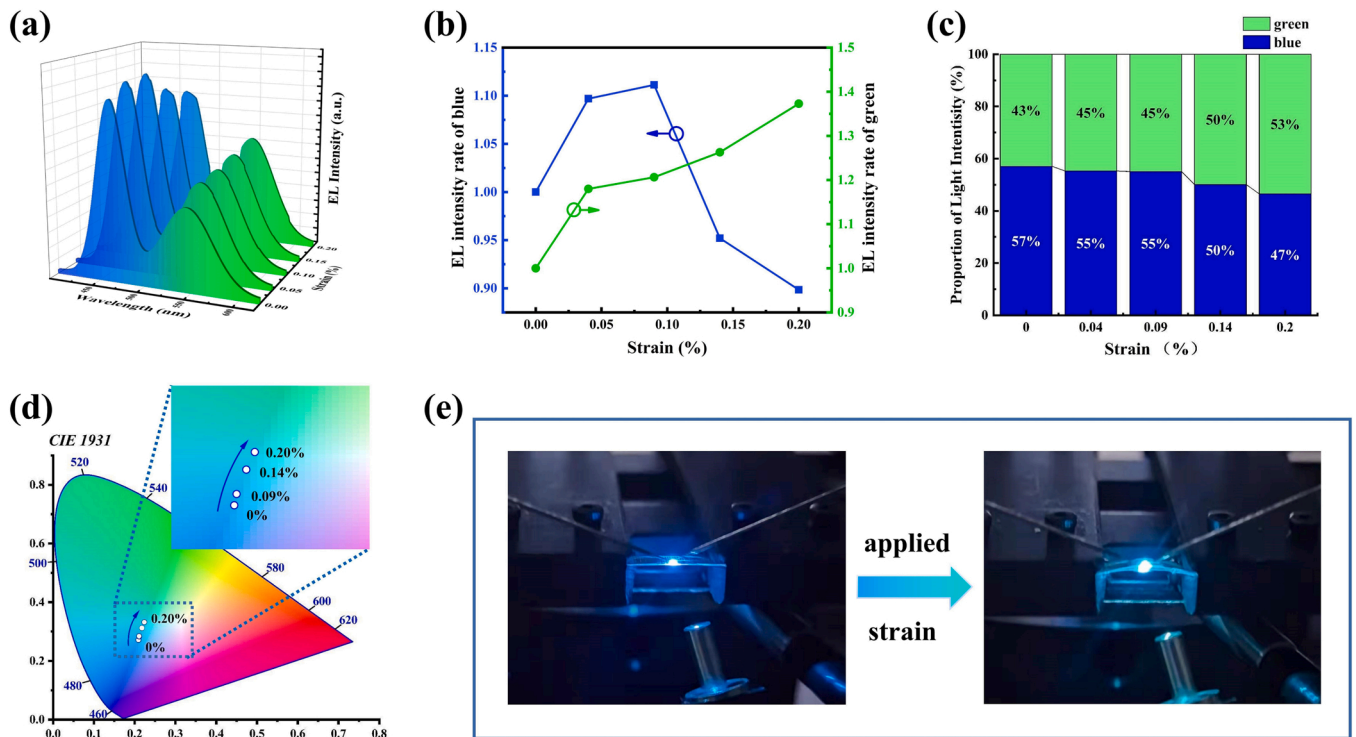


**Fig. 5.** (a) EL spectra of dual-wavelength Micro-LEDs at the current of 20 mA under different external strain. (b) EL intensity of blue peak and green peak under different strain conditions. (c) Integral intensity ratio of blue light and green light at different external strain. (d) CIE color coordinates of dual-wavelength InGaN/GaN MQWs Micro-LEDs under different external strain. (e) The luminous images at the strain of 0% and 0.20%, respectively.

luminous images at the strain of 0% and 0.20% are exhibited in Fig. 5(e), which are consistent with the results in CIE chromaticity diagram. The color change under different external bending strain can be interpreted as the piezo-phototronic modulation in the light emitting of blue and

green QWs, which is considered with the same mechanism as modulation in PL. However, the increase in the proportion of green light integral intensity in EL (~10%) in Fig. 5(c) is approximately twice than PL (~5%) in Fig. S1, indicating that higher color response is expected in

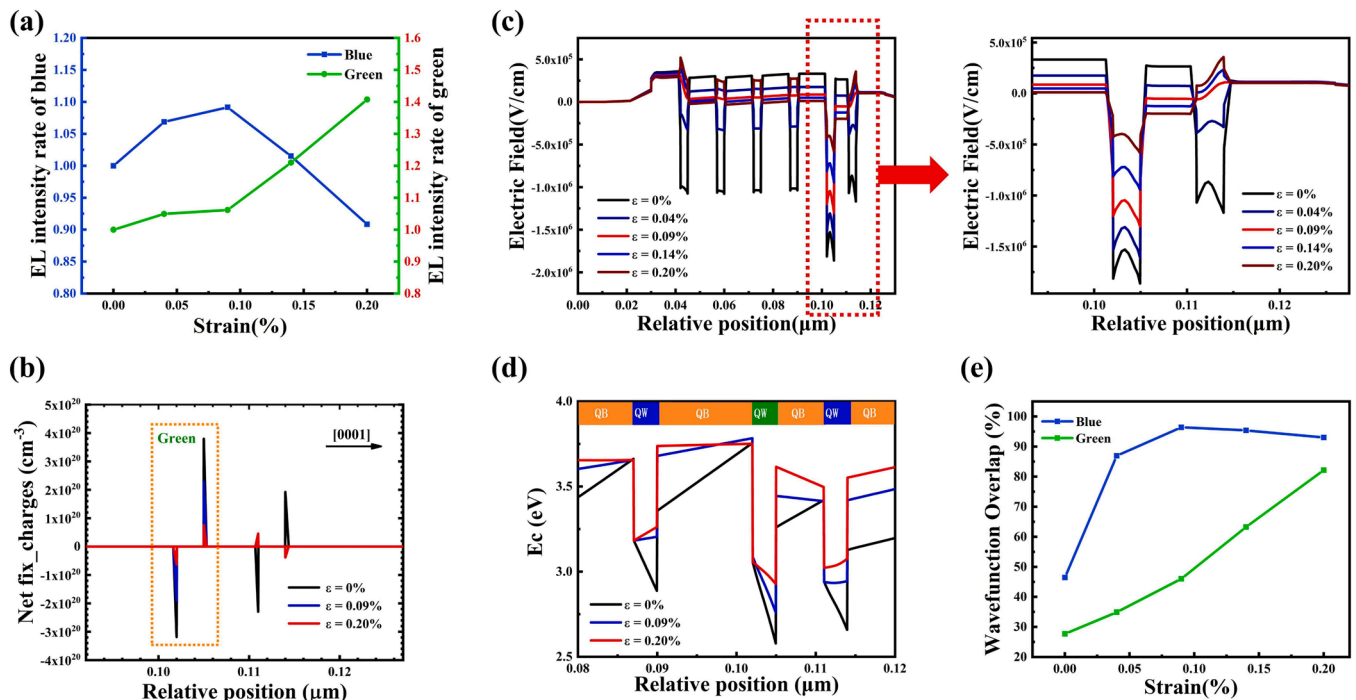


**Fig. 6.** (a) Simulation results of EL spectra under different external strain. (b) Distribution of interface polarized charges in blue and green QW under different external strain. (c) Electric field distribution in MQWs under different external strain. (d) Conduction band results in blue QW and green QW under different external strain. (e) Electron-hole wavefunction overlap in blue QW and green QW under different external strain.

electrical injection than optical pumping. Notably, the change of injection current density also significantly affects the spectral in Micro-LED [42,43]. At higher injection current of about 100 mA shown in Fig. S2, the intensity of green light becomes fully dominant compared to that of blue light. And when applied a 0.20% strain, the proportion of green light integral intensity increases about 10% as well, which is corresponding to the enhancement at the low injection current of 20 mA. Furthermore, with the application of external strain, the response current slightly increases in the I-V curve shown in Fig. S3. The strain-induced interface polarized charges change the built-in electric field, resulting in the modulation of band structure. Thus, the modulation of band structure might facilitate the injection of charge carriers [44]. Therefore, the strain-induced polarized charges modulate both the recombination in MQWs and the injection of carriers, which enables the significant strain-color response in dual-wavelength Micro-LED under electrical injection.

To deeply explore the physical mechanism of piezo-phototronic effect on the modulation of dual-wavelength Micro-LEDs, the simulation calculation of MQWs under electric injection is carried out by APSYS at different external strain. Considering the stress compensation effect of external stress on internal stress, the results of EL spectra simulation show well consistent trend with the experimental results as shown in Fig. 6(a). Due to the piezoelectric properties of wurtzite crystals along c-axis, piezoelectric polarized charges are compensated by strain-induced polarized charges under the c-axis compressive stress in MQWs [45]. In Fig. 6(b), before the critical strain of 0.09%, the net charges in the interface of green QW and blue QW both decreases. However, as the less lattice mismatch between GaN barrier and InGaN well in blue QW, the interfacial polarized charges slightly inverse at the excessive c-axis compressive stress. Simultaneously, the positive polarized charges in +c plane and the negative polarized charges in -c plane in green InGaN QW layer reduce to the minimum at the strain of 0.20%. These redistribution behaviors of piezoelectric polarized charges under various strain directly leads to the change of built-in piezoelectric polarization field in MQWs. With the increase of c-axis compressive strain, the electric field in each QW significantly reduces. Considering the carrier transport, the QWs that contribute to the light emission are mainly the last few wells near the p-GaN. It is exhibited that the built-in electric field consistently declines in green InGaN QW about two thirds. In the last blue InGaN QW layer, the electric field almost reduces to zero at the strain of 0.09% and then changes from negative to positive gradually at larger c-axis compressive strain as shown in Fig. 6(c). Correspondingly, the energy band structure is presented in Fig. 6(d) to further understand the modulation of color by external strain [46]. Owing to the reduced built-in electric field in both blue QW and green QW at a low external strain, the energy band tilt in InGaN QW decreases in Fig. 6(e), resulting in an enhancement of electron-hole wavefunction overlap ratio in Fig. 6(f). As a result, the radiative recombination increases in InGaN QWs, leading to the higher light emission of both blue and green light. The integral intensity ratio of green peak and blue peak slightly increases, which changes the display color of dual-wavelength Micro-LED. However, the reversal of the built-in electric field results in a reverse tilt of energy band in blue QW after a critical c-axis compressive strain, while the energy tilt further reduces in green QW (more details are shown in Fig. S4). This means the electron-hole wavefunction overlap ratio in blue QW and green QW changes in the opposite trend, and thus the green light further increases but the blue light decreases. In addition, the electron concentration in the last blue QW drops rapidly and the electron overshoot is effectively relieved as the external strain increases, as shown in Fig. S5. Therefore, the display color significantly changes under different external strain in dual-wavelength Micro-LEDs, exhibiting the strain-optical response characteristic.

#### 4. Conclusion

In summary, we have fabricated the blue and green dual-wavelength

Micro-LED arrays and demonstrated the color response characteristic of blue and green InGaN/GaN MQWs under external strain based on piezo-phototronic effect. Visually recognizable color change is observed in both PL and EL under different strain conditions in dual-wavelength Micro-LEDs. The green light intensity increases by 37% while the blue light decreases by 10% at the same strain about 0.20%, which realizes the integral intensity ratio change of green and blue light from 43:57–53:47. The display color shifts from light blue to turquoise with the increase of in-plane tensile strain. Furthermore, the physical mechanism of piezo-phototronic effect in blue QW and green QW is revealed by combining TRPL, modulation bandwidth experiments and AYSYS simulation. The difference in the energy band modulation of blue QW and green QW causes the different trends of radiative recombination in the two types of QWs, which finally results in the change of dual-wavelength spectra under different strain. This work provides a new method for the design of stress visualized and high spatial resolution optical stress sensor toward wearable electronics and human-machine interfaces.

#### CRediT authorship contribution statement

**Yu Yin:** Writing – original draft, Methodology. **Renfeng Chen:** Writing – original draft, Methodology. **Rui He:** Methodology. **Yiwei Duo:** Visualization. **Hao Long:** Conceptualization, Writing – review & editing. **Weiguo Hu:** Supervision. **Junyi Zhai:** Supervision. **Caofeng Pan:** Supervision. **Zihui Zhang:** Software. **Junxi Wang:** Supervision. **Jinmin Li:** Supervision. **Tongbo Wei:** Conceptualization, Writing – review & editing.

#### Declaration of Competing Interest

The authors declare that they have no known competing financial interests or personal relationships that could have appeared to influence the work reported in this paper.

#### Data Availability

Data will be made available on request.

#### Acknowledgements

This work was financially supported by the National Natural Science Foundation of China (Grants 52192614, 61974139 and 62135013), the National Key Research and Development Program of China (Grant 2019YFA0708203), Beijing Natural Science Foundation (No. 4222077) and Beijing Science and Technology Plan (No. Z221100002722019).

#### Appendix A. Supporting information

Supplementary data associated with this article can be found in the online version at [doi:10.1016/j.nanoen.2023.108283](https://doi.org/10.1016/j.nanoen.2023.108283).

#### References

- [1] J.H. Choi, Y.S. No, J.P. So, J.M. Lee, K.H. Kim, M.S. Hwang, S.H. Kwon, H.G. Park, A high-resolution strain-gauge nanolaser, *Nat. Commun.* 7 (2016) 11569, <https://doi.org/10.1038/ncomms11569>.
- [2] C. Wang, D. Hwang, Z. Yu, K. Takei, J. Park, T. Chen, B. Ma, A. Javey, User-interactive electronic skin for instantaneous pressure visualization, *Nat. Mater.* 12 (2013) 899, <https://doi.org/10.1038/nmat3711>.
- [3] T.Q. Trung, N.E. Lee, Flexible and stretchable physical sensor integrated platforms for wearable human-activity monitoring and personal healthcare, *Adv. Mater.* 28 (2016) 4338–4372, <https://doi.org/10.1002/adma.201504244>.
- [4] B. Zhou, Y. Li, D. Zhang, G. Zheng, K. Dai, L. Mi, C. Liu, C. Shen, Interfacial adhesion enhanced flexible polycarbonate/carbon nanotubes transparent conductive film for vapor sensing, *Compos. Commun.* 15 (2019) 80, <https://doi.org/10.1016/j.coco.2019.06.012>.
- [5] M. Stoppa, A. Chiolerio, Wearable electronics and smart textiles: a critical review, *Sensors* 14 (2014) 11957, <https://doi.org/10.3390/s140711957>.

- [6] S. Gong, W. Schwalb, Y. Wang, Y. Chen, Y. Tang, J. Si, B. Shirinzadeh, W. Cheng, A wearable and highly sensitive pressure sensor with ultrathin gold nanowires, *Nat. Commun.* 5 (2014) 3132, <https://doi.org/10.1038/ncomms4132>.
- [7] T. Yamada, Y. Hayamizu, Y. Yamamoto, Y. Yomogida, A. Izadi-Najafabadi, D. N. Futaba, K. Hata, A stretchable carbon nanotube strain sensor for human-motion detection, *Nat. Nanotechnol.* 6 (2011) 296, <https://doi.org/10.1038/nnano.2011.36>.
- [8] J. Mao, C.X. Zhao, L. Liu, Y.T. Li, D. Xiang, Y.P. Wu, H. Li, Adhesive, transparent, stretchable, and strain-sensitive hydrogel as flexible strain sensor, *Compos. Commun.* 25 (2021) 6, <https://doi.org/10.1016/j.coco.2021.100733>.
- [9] S. Mao, B. Chen, Y. Zheng, X. Li, Z. Huang, Y. Fu, Y. Lei, C. Wang, S. Qu, D. Peng, Dynamic limb-pressure visualization and measurement based on mechanoluminescent materials, *Chin. J. Lumin* 42 (2021) 397–403, <https://doi.org/10.37188/CJL.20210031>.
- [10] Y. Yuan, G. Giri, A.L. Ayzner, A.P. Zoombelt, S.C. Mannsfeld, J. Chen, D. Nordlund, M.F. Toney, J. Huang, Z. Bao, Ultra-high mobility transparent organic thin film transistors grown by an off-centre spin-coating method, *Nat. Commun.* 5 (2014) 3005, <https://doi.org/10.1038/ncomms4005>.
- [11] M.Z. Peng, Z. Li, C.H. Liu, Q. Zheng, X.Q. Shi, M. Song, Y. Zhang, S.Y. Du, J.Y. Zhai, Z.L. Wang, High-Resolution dynamic pressure sensor array based on Piezo-phototronic effect tuned photoluminescence imaging, *ACS Nano* 9 (2015) 3143, <https://doi.org/10.1021/acsnano.5b00072>.
- [12] S. Zhang, Z. Shi, J. Yuan, X. Gao, W. Cai, Y. Jiang, Y. Liu, Y. Wang, Membrane light-emitting diode flow sensor, *Adv. Mater. Technol.* -US 3 (2017), 1700285, <https://doi.org/10.1002/admt.201700285>.
- [13] J. Jing, X. An, Y. Luo, L. Chen, Z. Chu, K.H. Li, A compact optical pressure sensor based on a III-Nitride photonic chip with nanosphere-embedded PDMS, *ACS Appl. Electron. Mater.* 3 (2021) 1982, <https://doi.org/10.1021/acsaem.1c00130>.
- [14] X. An, Y. Luo, B. Yu, L. Chen, K.H. Li, A chip-scale gan-based optical pressure sensor with microdome-patterned polydimethylsiloxane (PDMS), *IEEE Electr. Device L* 42 (2021) 1532, <https://doi.org/10.1109/LED.2021.3103891>.
- [15] E. Vorathin, Z.M. Hafizi, N. Ismail, M. Loman, Review of high sensitivity fibre-optic pressure sensors for low pressure sensing, *Opt. Laser Technol.* 121 (2020), 105841, <https://doi.org/10.1016/j.optlastec.2019.105841>.
- [16] Y. Peng, M. Que, H.E. Lee, R. Bao, X. Wang, J. Lu, Z. Yuan, X. Li, J. Tao, J. Sun, J. Zhai, K.J. Lee, C. Pan, Achieving high-resolution pressure mapping via flexible GaN/ZnO nanowire LEDs array by piezo-phototronic effect, *Nano Energy* 58 (2019) 633, <https://doi.org/10.1016/j.nanoen.2019.01.076>.
- [17] C. Pan, L. Dong, G. Zhu, S. Niu, R. Yu, Q. Yang, Y. Liu, Z.L. Wang, High-resolution electroluminescent imaging of pressure distribution using a piezoelectric nanowire LED array, *Nat. Photonics* 7 (2013) 752, <https://doi.org/10.1038/nphoton.2013.191>.
- [18] X. Dai, Q. Hua, W. Sha, J. Wang, W. Hu, Piezo-phototronics in quantum well structures, *J. Appl. Phys.* 131 (2022), 010903, <https://doi.org/10.1063/5.0069663>.
- [19] L. Algieri, M.T. Todaro, F. Guido, V. Mastroradi, D. Desmaële, A. Qualtieri, C. Giannini, T. Sibillano, M.D. Vittorio, Flexible Piezoelectric energy-harvesting exploiting biocompatible aln thin films grown onto spin-coated polyimide layers, *ACS Appl. Energy Mater.* 1 (2018) 5203–5210, <https://doi.org/10.1021/acsaem.8b00820>.
- [20] J. Kang, D.K. Jeong, S. Ryu, Transparent, flexible piezoelectric nanogenerator based on GaN membrane using electrochemical lift-off, *ACS Appl. Mater. Interfaces* 9 (2017) 10637–10642, <https://doi.org/10.1021/acsaem.6b15587>.
- [21] C. Xie, M. Dan, G. Hu, N. Liu, Y. Zhang, Piezo-phototronic spin laser based on wurtzite quantum wells, *Nano Energy* 96 (2022), 107100, <https://doi.org/10.1016/j.nanoen.2022.107100>.
- [22] N. Laxmi, S. Routray, K.P. Pradhan, Effect of strain-modulated multiple quantum wells on carrier dynamics and spectral sensitivity of III-Nitride photosensitive devices, *IEEE Sens. J.* 20 (2020) 5204–5212, <https://doi.org/10.1109/JSEN.2020.2971005>.
- [23] Z.L. Wang, Progress in Piezotronics and Piezo-Phototronics, *Adv. Mater.* 24 (2012) 4632, <https://doi.org/10.1002/adma.201104365>.
- [24] W. Tian, Y. Wang, L. Chen, L. Li, Self-Powered nanoscale photodetectors, *Small* 13 (2017), 1701848, <https://doi.org/10.1002/sml.201701848>.
- [25] X. Huang, C. Du, Y. Zhou, C. Jiang, X. Pu, W. Liu, W. Hu, H. Chen, Z.L. Wang, Piezo-phototronic effect in a quantum well structure, *ACS Nano* 10 (2016) 5145, <https://doi.org/10.1021/acsnano.6b00417>.
- [26] R. Chen, Y. Yin, L. Wang, Y. Gao, R. He, J. Ran, J. Wang, J. Li, T. Wei, Strain modulated luminescence in green InGaN/GaN multiple quantum wells with microwire array by piezo-phototronic effect, *Opt. Lett.* 47 (2022) 6157–6160, <https://doi.org/10.1364/OL.477968>.
- [27] N.A. Dvorak, P. Ku, Low-Profile shear force tactile sensor based on optical methods, *IEEE Electr. Device L* 43 (2022) 1081, <https://doi.org/10.1109/LED.2022.3174096>.
- [28] J. Jiang, Q. Wang, B. Wang, J. Dong, Z. Li, X. Li, Y. Zi, S. Li, X. Wang, Direct lift-off and the piezo-phototronic study of InGaN/GaN heterostructure membrane, *Nano Energy* 59 (2019) 545, <https://doi.org/10.1016/j.nanoen.2019.02.066>.
- [29] L. Chen, K. Zhang, J. Dong, B. Wang, L. He, Q. Wang, M. He, X. Wang, The piezotronic effect in InGaN/GaN quantum-well based microwire for ultrasensitive strain sensor, *Nano Energy* 72 (2020) 4660, <https://doi.org/10.1016/j.nanoen.2020.10>.
- [30] J. Chen, J. Wang, K. Ji, B. Jiang, X. Cui, W. Sha, B. Wang, X. Dai, Q. Hua, L. Wan, W. Hu, Flexibles, stretchable, and transparent InGaN/GaN multiple quantum wells/polyacrylamide hydrogel-based light emitting diodes, *Nano Res.* 15 (2022) 5492, <https://doi.org/10.1007/s12274-022-4170-4>.
- [31] X. Luo, W. Song, F. Gao, J. Shi, C. Cheng, J. Guo, L. He, Q. Liu, Y. Yang, S. Li, Q. Wu, Strain-Modulated light emission properties in a single InGaN/GaN multiple-quantum-well microwire-based flexible light-emitting diode, *Adv. Eng. Mater.* 23 (2021), <https://doi.org/10.1002/adem.202001430>.
- [32] C. Du, C. Jiang, P. Zuo, X. Huang, X. Pu, Z. Zhao, Y. Zhou, L. Li, H. Chen, W. Hu, Z. L. Wang, Piezo-phototronic effect controlled dual-channel visible light communication (PVL) using InGaN/GaN multiquantum well nanopillars, *Small* 11 (2015) 6071, <https://doi.org/10.1002/sml.201502170>.
- [33] W.Z. Tawfik, S. Bae, S.B. Yang, T. Jeong, J.K. Lee, Stress engineering by controlling sapphire substrate thickness in 520 nm GaN-Based light-emitting diodes, *Appl. Phys. Express* 6 (2013), 122103, <https://doi.org/10.7567/APEX.6.122103>.
- [34] T. Wang, J. Bai, S. Sakai, J.K. Ho, Investigation of the emission mechanism in InGaN/GaN-based light-emitting diodes, *Appl. Phys. Lett.* 78 (2001) 2617, <https://doi.org/10.1063/1.1368374>.
- [35] C. Kisielowski, J. Kruger, S. Ruvimov, T. Suski, J.W. Ager, E. Jones, Z. LilientalWeber, M. Rubin, E.R. Weber, M.D. Bremser, R.F. Davis, Strain-related phenomena in GaN thin films, *Phys. Rev. B* 54 (1996) 17745, <https://doi.org/10.1103/PhysRevB.54.17745>.
- [36] S.-C. Tsai, C.-H. Lu, C.-P. Liu, Piezoelectric effect on compensation of the quantum-confined Stark effect in InGaN/GaN multiple quantum wells based green light-emitting diodes, *Nano Energy* 28 (2016) 373, <https://doi.org/10.1016/j.nanoen.2016.08.061>.
- [37] J. Mo, Q. Hua, W. Sha, M. Yao, J. Wang, L. Wan, J. Zhai, T. Lin, W. Hu, Dynamic piezo-phototronic effect in InGaN/GaN multiple quantum wells, Superlattices Microstruct. 155 (2021), 106926, <https://doi.org/10.1016/j.spmi.2021.106926>.
- [38] D.W. Yang, K. Lee, S. Jang, W.J. Chang, S.H. Kim, J.H. Lee, G.C. Yi, W.I. Park, Large Wavelength response to pressure enabled in InGaN/GaN Microcrystal LEDs with 3D architectures, *ACS Photonics* 7 (2020) 1122, <https://dx.doi.org/10.1021/acsp Photonics.0c00251>.
- [39] S.-W. Feng, Y.-C. Cheng, Y.-Y. Chung, C.C. Yang, M.-H. Mao, Y.-S. Lin, K.-J. Ma, J.-I. Chyi, Multiple-component photoluminescence decay caused by carrier transport in InGaN/GaN multiple quantum wells with indium aggregation structures, *Appl. Phys. Lett.* 80 (2002) 4375, <https://doi.org/10.1063/1.1484546>.
- [40] X. Zou, J. Dong, K. Zhang, W. Lin, M. Guo, W. Zhang, The piezotronic effect on carrier recombination processes in InGaN/GaN multiple quantum wells microwire, *Nano Energy* 87 (2021), 106145, <https://doi.org/10.1016/j.nanoen.2021.106145>.
- [41] M. Monavarian, A. Rashidi, A.A. Aragon, M. Nami, S.H. Oh, S.P. DenBaars, D. Feezell, Trade-off between bandwidth and efficiency in semipolar (2021) InGaN/GaN single- and multiple-quantum-well light-emitting diodes, *Appl. Phys. Lett.* 112 (2018), 191102, <https://doi.org/10.1063/1.5032115>.
- [42] J. Zhao, Y. Yin, R. He, R. Chen, S. Zhang, H. Long, J. Wang, T. Wei, GaN-based parallel micro-light-emitting diode arrays with dual-wavelength In<sub>x</sub>Ga<sub>1-x</sub>N/GaN MQWs for visible light communication, *Opt. Express* 30 (2022) 18461, <https://doi.org/10.1364/OE.452679>.
- [43] H.B. Yu, M.H. Memon, H.F. Jia, H.C. Zhang, M. Tian, S. Fang, D.H. Wang, Y. Kang, S.D. Xiao, S.B. Long, H.D. Sun, A 10 × 10 deep ultraviolet light-emitting micro-LED array, *J. Semicond.* 43 (2022), 062801, <https://doi.org/10.1088/1674-4926/43/6/062801>.
- [44] W. Song, X. Wang, C. Xia, R. Wang, L. Zhao, D. Guo, H. Chen, J. Xiao, S. Su, S. Li, Improved photoresponse of a-axis GaN microwire/p-polymer hybrid photosensor by the piezo-phototronic effect, *Nano Energy* 33 (2017) 272–279, <https://doi.org/10.1016/j.nanoen.2017.01.032>.
- [45] W. Sha, Q. Hua, J. Wang, Z. Cong, X. Cui, K. Ji, X. Dai, B. Wang, W. Guo, W. Hu, Enhanced Photoluminescence of Flexible InGaN/GaN Multiple Quantum Wells on Fabric by Piezo-Phototronic Effect, *ACS Appl. Mater. Interfaces* 14 (2022) 3000, <https://doi.org/10.1021/acsaem.1c12835>.
- [46] S. Lu, J. Li, K. Huang, G. Liu, Y. Zhou, D. Cai1, R. Zhang, J. Kang, Designs of InGaN Micro-LED structure for improving quantum efficiency at low current density, *Nanoscale Res. Lett.* 16 (2021) 99, <https://doi.org/10.1186/s11671-021-03557-4>.



**Yin Yu** is a graduate student in Xiamen University. He received his B.S. degree in materials Physics from Taiyuan University of Technology. He is mainly engaged in the research of optoelectronic devices based on wide-band gap semiconductor materials.



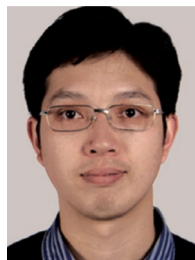
**Renfeng Chen** is a graduate student in the Institute of Semiconductors, Chinese Academy of Sciences. He received B.S. degree in Applied Physics from Hebei University of Technology. His research mainly focuses on GaN-based optoelectronic devices and Piezo-photonics.



**Dr. Junyi Zhai** received his Ph.D. from Virginia Polytechnic Institute and State University in 2009. Now he is Professor at Beijing Institute of Nanoenergy and Nanosystems, Chinese Academy of Sciences. His main research interest and activities are: micro/nano piezoelectric semiconductors, sensors and self-power systems.



**Rui He** is a graduate student in the Institute of Semiconductors, Chinese Academy of Sciences. She received her B.S. degree in Applied Physics from University of Science and Technology Beijing. Her research mainly focuses on the research of optoelectronic integrated devices based on wide bandgap semiconductor materials.



**Caofeng Pan** received his B.S. degree (2005) and his Ph.D. (2010) in Materials Science and Engineering from Tsinghua University, China. He then joined in the group of Professor Zhong Lin Wang at the Georgia Institute of Technology as a postdoctoral fellow. He is currently a professor and a group leader at Beijing Institute of Nanoenergy and Nanosystems, Chinese Academy of Sciences since 2013. His main research interests focus on the fields of piezotronics/piezo-phototronics for fabricating new electronic and optoelectronic devices and self-powered nanosystems.



**Yiwei Duo** is a master degree candidate in the Institute of Semiconductors, Chinese Academy of Sciences. He received his B.E. degree in New Energy Science and Engineering from Qingdao University. His research mainly focuses on van der Waals epitaxial growth of III-nitride semiconductor materials and the fabrication of optoelectronic devices based on these materials.



**Zihui Zhang**, graduated from Singapore Nanyang Technological University and obtained a doctor's degree, and then stayed in the school as a researcher of Nanyang Technological University. At present, he is serving as a professor of Guangdong University of Technology. The main research is the third generation semiconductor devices, semiconductor device physics, chip design and simulation technology and industrialization promotion.



**Hao Long** is currently an associate professor in department of Microelectronics and Integrated Circuits, Xiamen University. He received the B.S. and Ph.D. degrees in physics from Peking University, Beijing, China, in 2008 and 2013, respectively. His research interests focus on semiconductor optoelectronics, light-emitting diodes, and semiconductor visible light lasers.



**Junxi Wang** is currently a professor in the Materials Physics and Chemistry, Institute of Semiconductors, Chinese Academy of Sciences. He received his bachelor degree in physics from Northwestern university in 1998 and his doctor degree in engineering from Institute of Semiconductors, Chinese Academy of Sciences in 2003. His research interests focus on wide gap semiconductor material epitaxy, deep ultraviolet light-emitting diode (DUV-LED) device, advanced semiconductor materials and their applications.



**Prof. Weiguo Hu** is a professor and principal investigator at the Beijing Institute of Nanoenergy and Nanosystems, Chinese Academy of Science (CAS), China. He received his PhD degree from the Institute of Semiconductors, CAS, in 2007. His research focuses on gallium nitride-based piezotronic/piezophotonic devices and wearable self-powered nanosystems. He has authored more than 70 peer-reviewed journal articles in these fields.



**Jinmin Li** received his bachelor degree in semiconductor physics and device engineering from Xi'an Jiaotong University in 1982, his master degree in semiconductor materials and device physics from the 13th Institute of Electronics, Ministry of Information Industry in 1984, and his doctor degree in optics from Xi'an Institute of Optics and Precision Mechanics, Chinese Academy of Sciences in 1991. His research interests focus on compound semiconductor single crystal materials and nitride materials epitaxy. He has made outstanding contributions to the research and development of optoelectronic devices, and optics for optical communications and solid-state lighting.



**Tongbo Wei** is currently a professor in the Materials Physics and Chemistry, Institute of Semiconductors, Chinese Academy of Sciences. He received his doctoral degree in engineering from the Institute of Semiconductors, Chinese Academy of Sciences in July 2007. His research interests focus on wide bandgap semiconductor materials and devices, new micro-nano photoelectronic devices, deep ultraviolet light emitting devices, and nitride growth on two-dimensional materials.